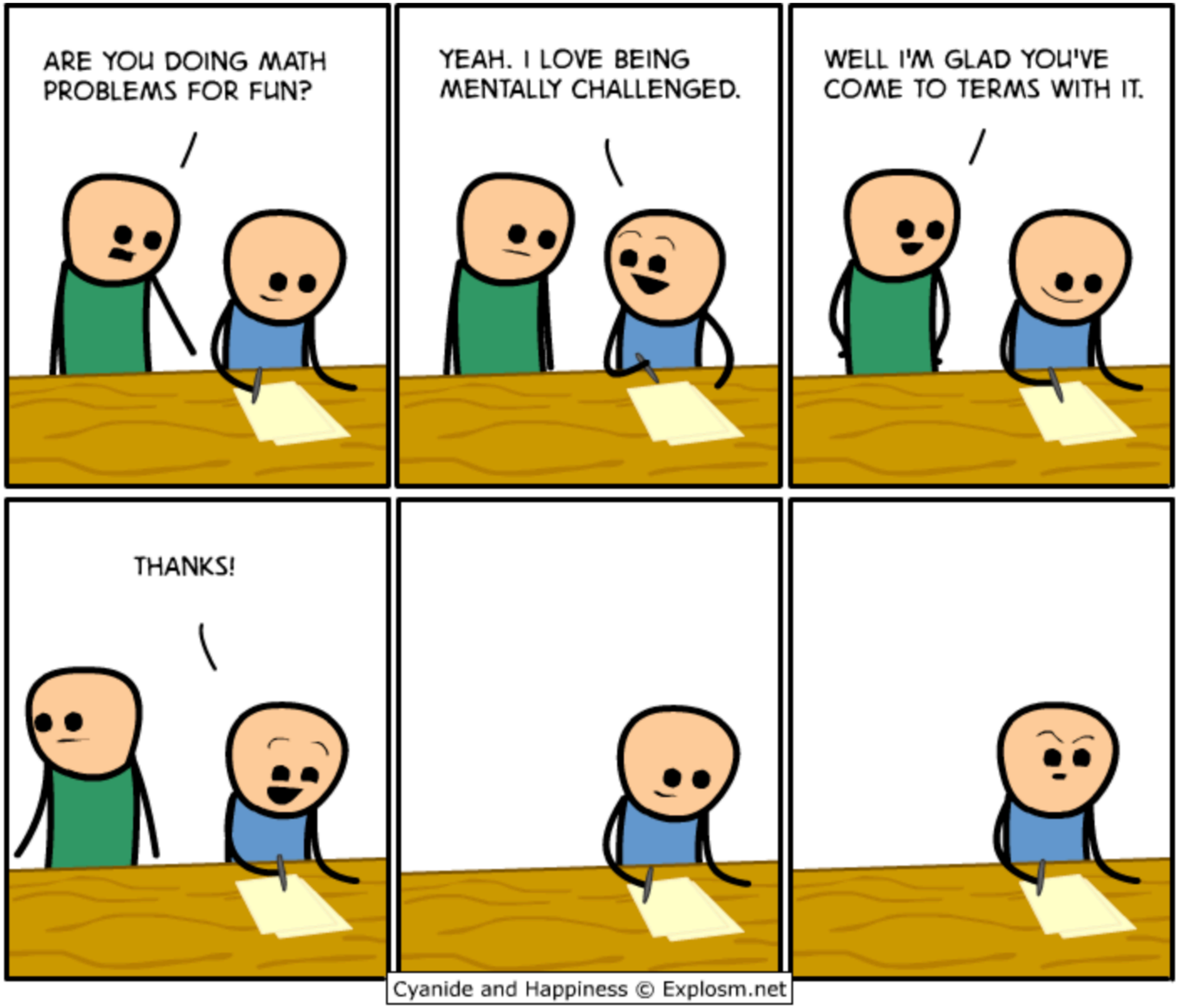

2013.09.03
by Rob DenBleyker
@RobDenBleyker

’Bout me: I am ‘Indra’!

1. B.Sc. and M.Sc. in Physics (2015–2020)
2. Ph.D. in Applied Math (2021–2024)
3. First postdoc in Applied Math (2024–2025)
4. Current postdoc in Mathematical Neuroscience (2025—Present)

যাদবপুর বিশ্ববিদ্যালয়
JADAVPUR UNIVERSITY

TE KUNENGA KI PŪREHUROA | MASSEY UNIVERSITY
UNIVERSITY OF NEW ZEALAND

University College Dublin
An Coláiste Ollscoile, Baile Átha Cliath

Mathematical Neuroscience group

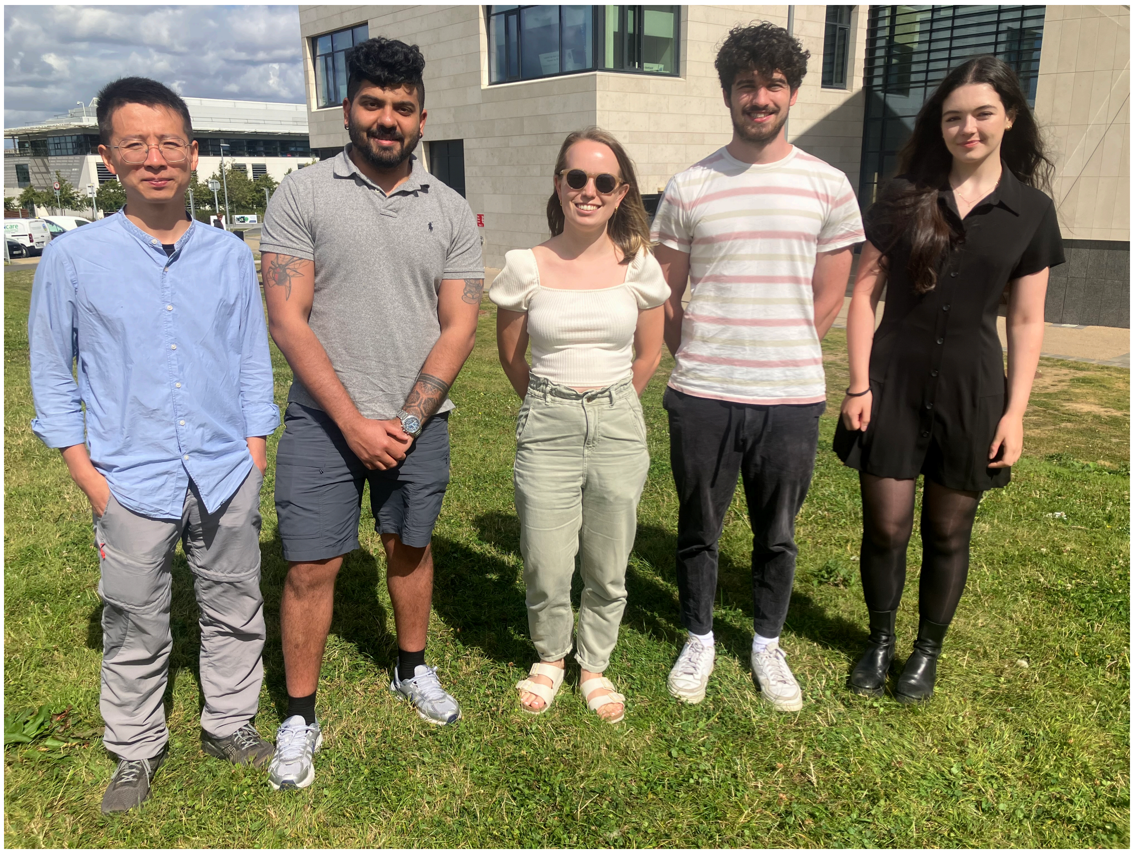

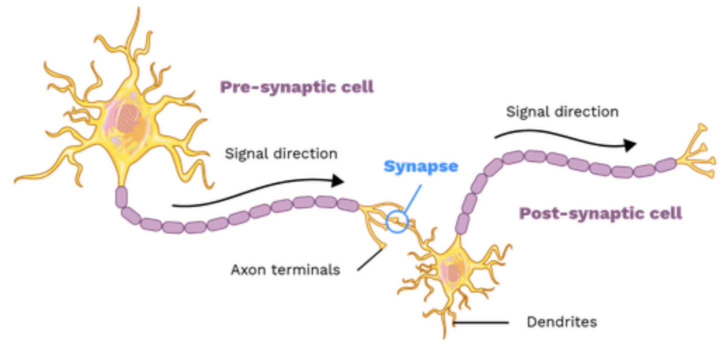

Fig. Coupled neurons
(theory.labster.com/synapses/)

Investigating robust chaos in piecewise-linear maps

Indranil Ghosh
School of Mathematics and Statistics, University College Dublin, Ireland
David J.W. Simpson
School of Mathematical and Computational Sciences, Massey University, New Zealand

October 22, 2025

MARSDEN FUND
TE PŪTEA RANGAHAU A MARSDEN
ROYAL SOCIETY TE APĀRANGI

Why is it important?

1. These maps have applications in designing secure encryption schemes (one of the main motivations that drives me!).

2. Investigating chaos regions might let engineers design proper fail-safes in switched systems in avionics, for example!

3. Prevention of undesirable chaotic regimes while designing DC-DC power converters and inverters.

4. Many more "…, which this margin is too small to contain."

Border-collision normal form

- Piecewise-linear maps arise when modeling systems with switches, thresholds and other abrupt events.
- In our project, we study the two-dimensional *border-collision normal form* (Nusse & Yorke, 1992), given by

$$f_\xi(x,y) = \begin{cases} \begin{bmatrix} \tau_L & 1 \\ -\delta_L & 0 \end{bmatrix} \begin{bmatrix} x \\ y \end{bmatrix} + \begin{bmatrix} 1 \\ 0 \end{bmatrix}, & x \le 0, \\ \begin{bmatrix} \tau_R & 1 \\ -\delta_R & 0 \end{bmatrix} \begin{bmatrix} x \\ y \end{bmatrix} + \begin{bmatrix} 1 \\ 0 \end{bmatrix}, & x \ge 0. \end{cases}$$

- Here $(x,y) \in \mathbb{R}^2$, and $\xi = (\tau_L, \delta_L, \tau_R, \delta_R) \in \mathbb{R}^4$ are the parameters.

Phase portrait of a chaotic attractor

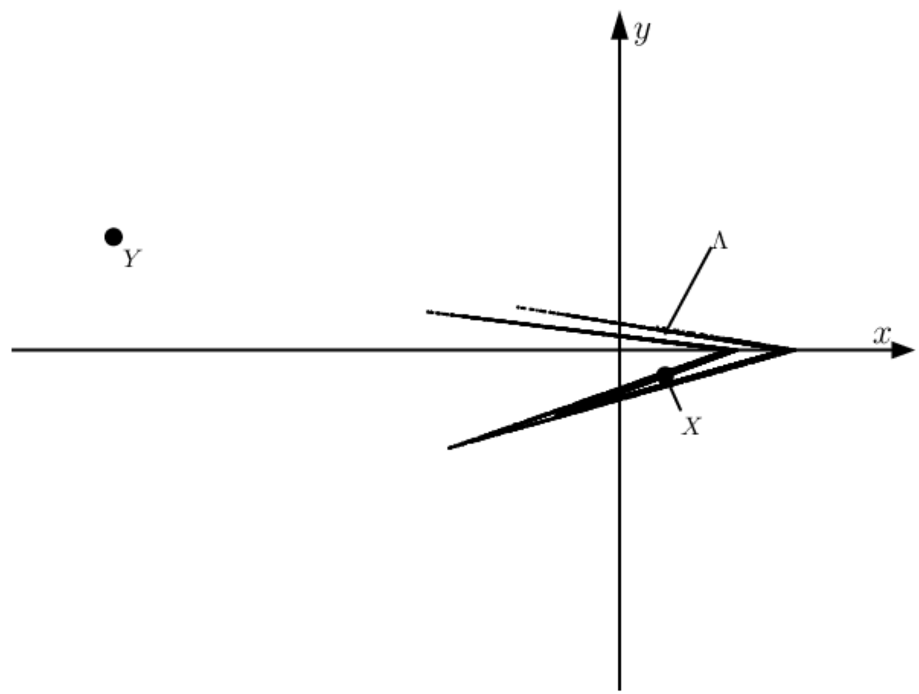

Figure: A sketch of the phase portrait of f_ξ with $\xi \in \Phi_{\mathrm{BYG}}$.

Renormalisation operator

- Renormalisation involves showing that, for some members of a family of maps, a higher iterate or induced map is conjugate to different member of this family of maps.
- Although the second iterate f_ξ^2 has four pieces, relevant dynamics arise in only two of these. We have

$$f_\xi^2(x,y) = \begin{cases} \begin{bmatrix} \tau_L\tau_R - \delta_L & \tau_R \\ -\delta_R\tau_L & -\delta_R \end{bmatrix} \begin{bmatrix} x \\ y \end{bmatrix} + \begin{bmatrix} \tau_R + 1 \\ -\delta_R \end{bmatrix}, & x \le 0, \\ \begin{bmatrix} \tau_R^2 - \delta_R & \tau_R \\ -\delta_R\tau_R & -\delta_R \end{bmatrix} \begin{bmatrix} x \\ y \end{bmatrix} + \begin{bmatrix} \tau_R + 1 \\ -\delta_R \end{bmatrix}, & x \ge 0. \end{cases}$$

- Now f_ξ^2 can be transformed to $f_{g(\xi)}$, where g is the *renormalisation operator* (Ghosh & Simpson, 2022.) $g : \mathbb{R}^4 \to \mathbb{R}^4$, given by

$$\left(\tilde{\tau}_L, \tilde{\delta}_L, \tilde{\tau}_R, \tilde{\delta}_R\right) = \left(\tau_R^2 - 2\delta_R, \delta_R^2, \tau_L\tau_R - \delta_L - \delta_R, \delta_L\delta_R\right)$$

Renormalisation operator

- We perform a coordinate change to put f_ξ^2 in the normal form :

$$\begin{bmatrix}\tilde{x}' \\ \tilde{y}'\end{bmatrix} = \begin{cases} \begin{bmatrix}\tilde{\tau}_L & 1 \\ -\tilde{\delta}_L & 0\end{bmatrix}\begin{bmatrix}\tilde{x} \\ \tilde{y}\end{bmatrix} + \begin{bmatrix}1 \\ 0\end{bmatrix}, & \tilde{x} \le 0, \\ \begin{bmatrix}\tilde{\tau}_R & 1 \\ -\tilde{\delta}_R & 0\end{bmatrix}\begin{bmatrix}\tilde{x} \\ \tilde{y}\end{bmatrix} + \begin{bmatrix}1 \\ 0\end{bmatrix}, & \tilde{x} \ge 0. \end{cases}$$

Results

- We consider the parameter region

$$\Phi = \left\{ \xi \in \mathbb{R}^4 \middle| \tau_L > \delta_L + 1, \delta_L > 0, \tau_R < -(\delta_R + 1), \delta_R > 0 \right\}.$$

- Let

$$\phi^+(\xi) = \zeta_0 = \delta_R - (\tau_R + \delta_L + \delta_R - (1 + \tau_R)\lambda_L^u)\lambda_L^u.$$

- The stable and the unstable manifolds of the fixed point Y intersect if and only if $\phi^+(\xi) \leq 0$.
- The attractor is often destroyed at $\phi^+(\xi) = 0$ which is a homoclinic bifurcation (Banerjee, Yorke & Grebogi, 1998), and thus focused their attention on the region

$$\Phi_{\mathrm{BYG}} = \left\{ \xi \in \Phi \middle| \phi^+(\xi) > 0 \right\}.$$

Results

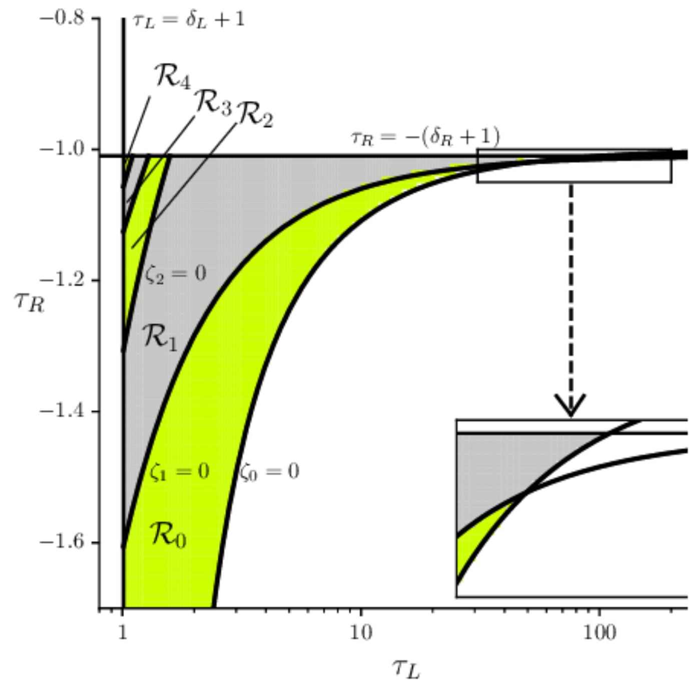

Figure: The sketch of two-dimensional cross-section of Φ_{BYG} when $\delta_L = \delta_R = 0.01$.

Results

Theorem (Ghosh & Simpson, 2022)

The $\mathcal{R}_n$ are non-empty, mutually disjoint, and converge to the fixed point $(1, 0, -1, 0)$ as $n \to \infty$. Moreover,

$$\Phi_{\mathrm{BYG}} \subset \bigcup_{n=0}^{\infty} \mathcal{R}_n.$$

Let,

$$\Lambda(\xi) = \mathrm{cl}(W^u(X)).$$

Theorem (Ghosh & Simpson, 2022)

For the map f_ξ with any $\xi \in \mathcal{R}_0$, $\Lambda(\xi)$ is bounded, connected, and invariant. Moreover, $\Lambda(\xi)$ is chaotic (positive Lyapunov exponent).

Results

Theorem (Ghosh & Simpson, 2022)

For any $\xi \in \mathcal{R}_n$ *where* $n \geq 0$, $g^n(\xi) \in \mathcal{R}_0$ *and there exist mutually disjoint sets* $S_0, S_1, \ldots, S_{2^n-1} \subset \mathbb{R}^2$ *such that* $f_\xi(S_i) = S_{(i+1) \textit{ mod } 2^n}$ *and*

$$f_\xi^{2^n}|_{S_i} \text{ is affinely conjugate to } f_{g^n(\xi)}|_{\Lambda(g^n(\xi))}$$

for each $i \in \{0, 1, \ldots, 2^n - 1\}$. *Moreover,*

$$\bigcup_{i=0}^{2^n-1} S_i = \mathrm{cl}(W^u(\gamma_n)),$$

where γ_n *is a saddle-type periodic solution of our map* f_ξ *having the symbolic itinerary* $\mathcal{F}^n(R)$ *given by Table 1.*

Results

n	$\mathcal{F}^n(\mathcal{W})$
0	R
1	LR
2	$RRLR$
3	$LRLRRRLR$
4	$RRLRRRLRLRLRRRLR$

Table: The first 5 words in the sequence generated by repeatedly applying the substitution rule $(L, R) \mapsto (RR, LR)$ to $\mathcal{W} = R$.

Results

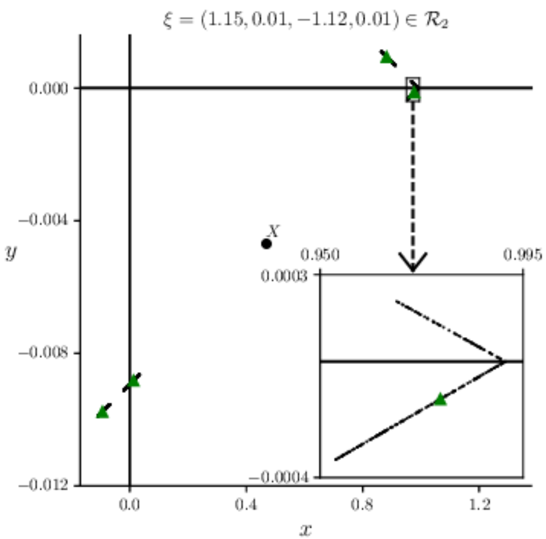
$\xi = (1.15, 0.01, -1.12, 0.01) \in \mathcal{R}_2$
0.000
−0.004
−0.008
−0.012
0.0
0.4
0.8
1.2
x
y
X
0.950
0.995
0.0003
−0.0004

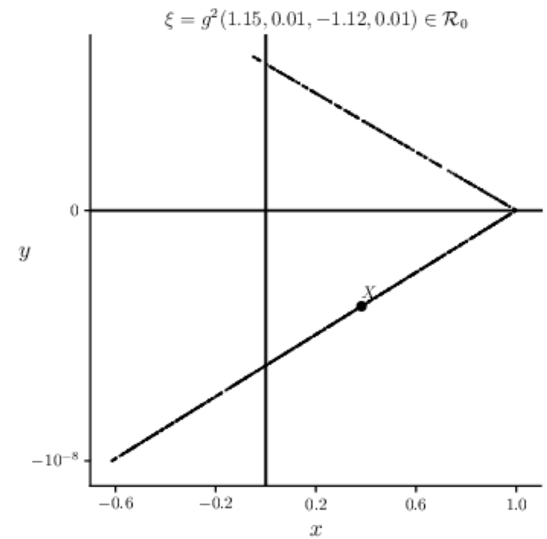
$\xi = g^2(1.15, 0.01, -1.12, 0.01) \in \mathcal{R}_0$
0
-10^{-8}
−0.6
−0.2
0.2
0.6
1.0
x
y
X

Devaney Chaos

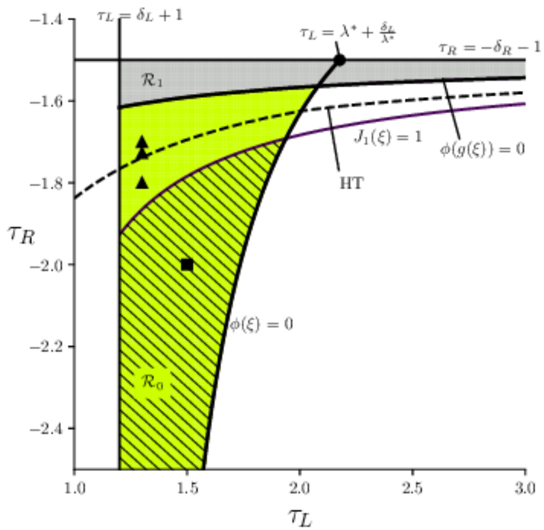

(a) $\delta_L = 0.2$, $\delta_R = 0.5$

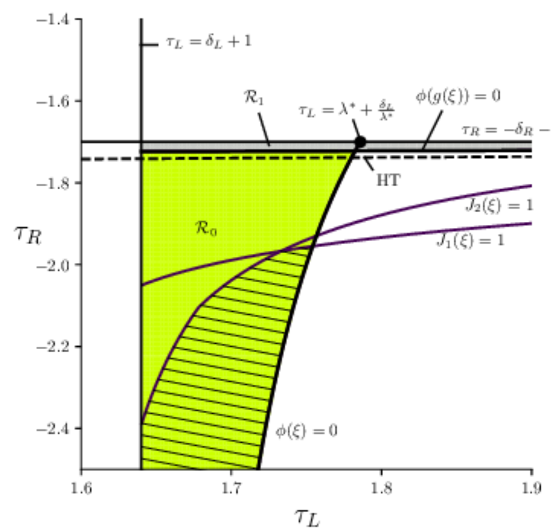

(b) $\delta_L = 0.64$ and $\delta_R = 0.7$

Devaney Chaos

Theorem (Ghosh & Simpson, 2022)

Let $\xi \in \Phi_{\mathrm{BYG}}$ *and suppose* $J_1(\xi) > 1$ *and* $\lambda_L^s + |\lambda_R^s| < 1$. *Then* $W^s(X)$ *is dense in a triangular region containing* Λ.

Theorem (Ghosh & Simpson, 2022)

Let $\xi \in \Phi_{\mathrm{BYG}}$ *and suppose* $J_1(\xi) > 1$ *and* $J_2(\xi) < 1$. *Then,* f_ξ *is chaotic in the sense of Devaney on* Λ.

Generalised parameter region

Now we consider the more generalised parameter region considering the orientation-reversing and non-invertible cases,

$$\Phi = \left\{ \xi \in \mathbb{R}^4 \;\middle|\; \tau_L > |\delta_L + 1|, \tau_R < -|\delta_R + 1| \right\}.$$

Typical phase portraits

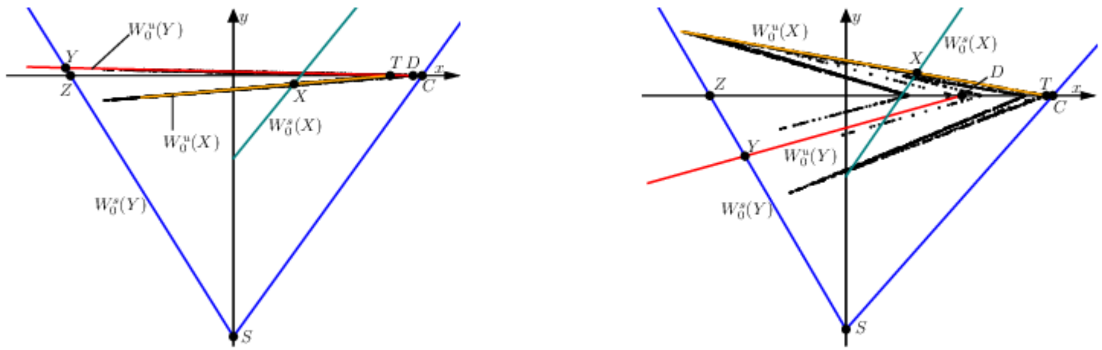

(a) $\delta_L > 0, \delta_R > 0$ (b) $\delta_L < 0, \delta_R < 0$

Figure: Typical phase portraits of the chaotic attractor for the invertible case ($\delta_L \delta_R > 0$).

Typical phase portraits

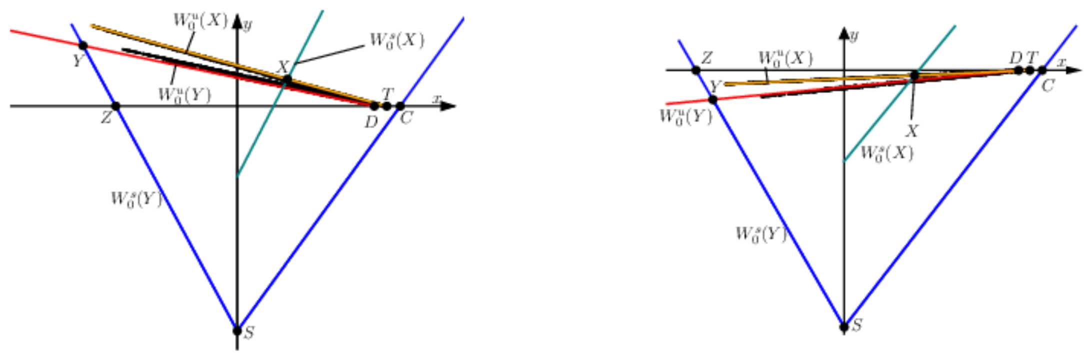

(a) $\delta_L > 0, \delta_R < 0$ (b) $\delta_L < 0, \delta_R > 0$

Figure: Typical phase portraits of the chaotic attractor for the non-invertible case ($\delta_L \delta_R < 0$).

Invariant expanding cones

Chaos in Φ_{BYG} can be proved by constructing an invariant expanding cone in tangent space (Glendinning & Simpson, 2021). We have extended this to Φ.

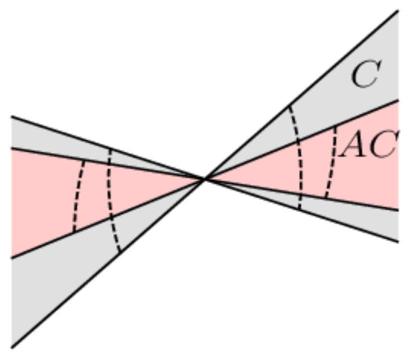

Figure: A sketch of an invariant expanding cone C and its image $AC = \{Av | v \in C\}$, given $A \in \mathbb{R}^{2\times 2}$.

Robust Chaos in a generalised setting

Theorem (Ghosh, McLachlan, & Simpson, 2023)

For any $\xi \in \Phi_{\mathrm{trap}} \cap \Phi_{\mathrm{cone}}$, the normal form f_ξ has a topological attractor with a positive Lyapunov exponent.

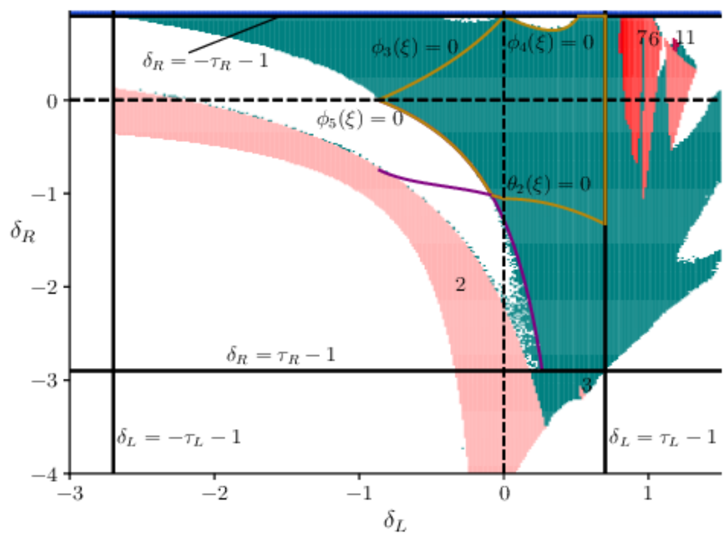

Figure: A 2D slice of $\Phi_{\mathrm{trap}} \cap \Phi_{\mathrm{cone}} \subset \mathbb{R}^4$.

The orientation-reversing case

- Let

$$\Phi^{(2)} = \{\xi \in \Phi \mid \delta_L < 0, \delta_R < 0\} \,,$$

  be the subset of Φ for which the BCNF is orientation-reversing.
- The attractor Λ which is again a closure of the unstable manifold of X faces a crisis at $\zeta_0^{(2)} = 0$ where

$$\zeta_0^{(2)} = \phi^-(\xi) = \delta_R - (\delta_R + \tau_R - (1 + \lambda_R^u)\lambda_L^u)\lambda_L^u \,.$$

The orientation-reversing case

- Now, $\xi \in \Phi^{(2)}$ implies $g(\xi) \in \Phi^{(1)}$, so we again use the preimages of $\phi^+(\xi) = 0$ under g to define the region boundaries: Specifically we let

$$\mathcal{R}_0^{(2)} = \left\{ \xi \in \Phi^{(2)} \,\middle|\, \phi^-(\xi) > 0, \phi^+(g(\xi)) \le 0, \alpha(\xi) < 0 \right\},$$
$$\mathcal{R}_n^{(2)} = \left\{ \xi \in \Phi^{(2)} \,\middle|\, \phi^+\left(g^n(\xi)\right) > 0, \phi^+\left(g^{n+1}(\xi)\right) \le 0, \alpha(\xi) < 0 \right\}, \qquad \text{for all } n \ge 1.$$

where

$$\alpha(\xi) = \tau_L \tau_R + (\delta_L - 1)(\delta_R - 1).$$

- This brings us to the proposition

Proposition (Ghosh, McLachlan, & Simpson, 2024)

If $\xi \in \mathcal{R}_n^{(2)}$ with $n \ge 1$, then $g(\xi) \in \mathcal{R}_{n-1}^{(1)}$.

The orientation-reversing case

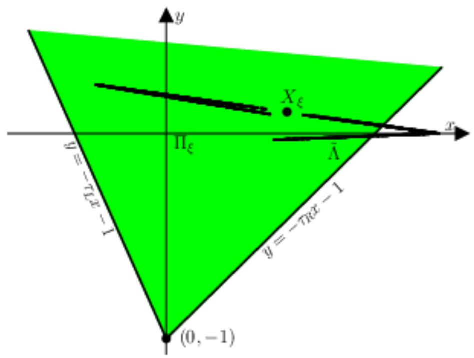

(a) $\xi = \xi_{\mathrm{ex}}^{(2)} \in \mathcal{R}_1^{(2)}$

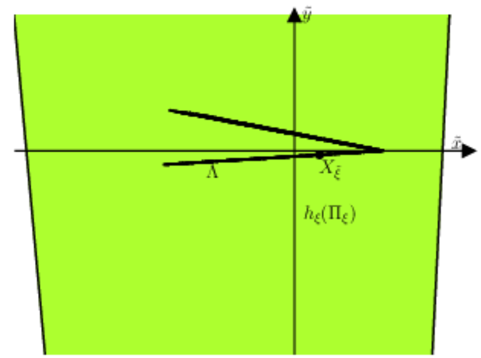

(b) $\xi = g(\xi_{\mathrm{ex}}^{(2)}) \in \mathcal{R}_0^{(1)}$

The non-invertible case $\delta_L > 0, \delta_R < 0$

- Let

$$\Phi^{(3)} = \{\xi \in \Phi \mid \delta_L > 0, \delta_R < 0\},$$

meaning the map is invertible.

- In this region an attractor can be destroyed by crossing the homoclinic bifurcation $\phi^+(\xi) = 0$ or the heteroclinic bifurcation $\phi^-(\xi) = 0$.
- we define

$$\phi_{\min}(\xi) = \min[\phi^+(\xi), \phi^-(\xi)].$$

and

$$\mathcal{R}_n^{(3)} = \left\{\xi \in \Phi^{(3)} \,\middle|\, \phi_{\min}\left(g^n(\xi)\right) > 0,\, \phi_{\min}\left(g^{n+1}(\xi)\right) \le 0,\, \alpha(\xi) < 0\right\},$$

for all $n \ge 0$.

The non-invertible case $\delta_L > 0, \delta_R < 0$

- This brings us to a new proposition:

Proposition (Ghosh, McLachlan, & Simpson, 2024)
If $\xi \in \mathcal{R}_n^{(3)}$ *with* $n \geq 1$*, then* $g(\xi) \in \mathcal{R}_{n-1}^{(3)}$.

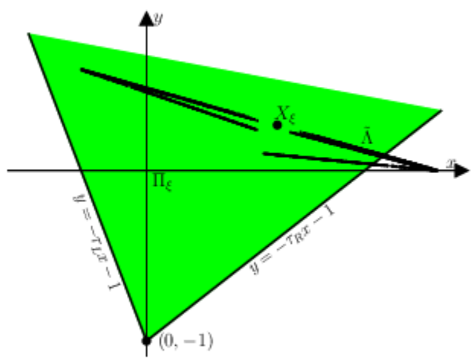

(a) $\xi = \xi_{\rm ex}^{(3)} \in \mathcal{R}_1^{(3)}$

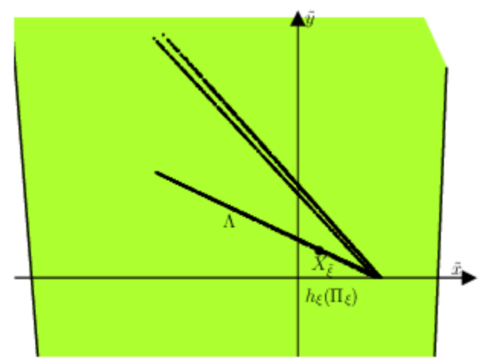

(b) $\xi = g(\xi_{\rm ex}^{(3)}) \in \mathcal{R}_0^{(3)}$

The non-invertible case $\delta_L < 0, \delta_R > 0$

- It remains for us to consider

$$\Phi^{(4)} = \{\xi \in \Phi \mid \delta_L < 0, \delta_R > 0\},$$

  where the BCNF is again non-invertible.
- In this region the attractor is usually destroyed before the boundaries $\phi^+(\xi) = 0$ and $\phi^-(\xi) = 0$ in a heteroclinic bifurcation that cannot be characterised by an explicit condition on the parameter values.
- Despite the extra complexities in $\Phi^{(4)}$ it still appears that renormalisation is helpful for explaining the bifurcation structure. Let

$$\mathcal{R}_0^{(4)} = \left\{\xi \in \Phi^{(4)} \,\middle|\, \phi_{\min}(\xi) > 0,\ \phi_{\min}(g(\xi)) \le 0,\ \alpha(\xi) < 0\right\}.$$

$$\mathcal{R}_n^{(4)} = \left\{\xi \in \Phi^{(4)} \,\middle|\, \phi_{\min}(g^n(\xi)) > 0,\ \phi_{\min}(g^{n+1}(\xi)) \le 0,\ \alpha(\xi) < 0, \alpha(g(\xi)) < 0\right\}.$$

The non-invertible case $\delta_L < 0, \delta_R > 0$

- This brings us to the new propostion:

Proposition (Ghosh, McLachlan, & Simpson, 2024)
If $\xi \in \mathcal{R}_n^{(4)}$ *with* $n \geq 1$, *then* $g(\xi) \in \mathcal{R}_{n-1}^{(3)}$.

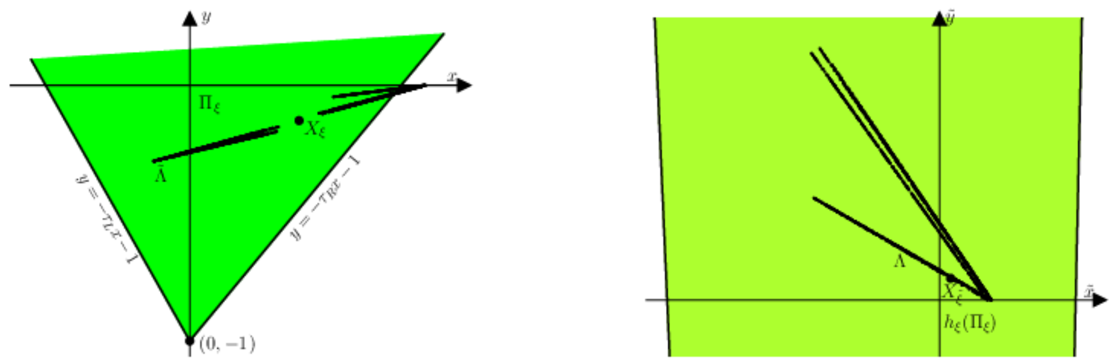

(a) $\xi = \xi_{\text{ex}}^{(4)} \in \mathcal{R}_1^{(4)}$

(b) $\xi = g(\xi_{\text{ex}}^{(4)}) \in \mathcal{R}_0^{(3)}$

Numerics

- We verify these bifurcation structures numerically by using Eckstein's greatest common divisor algorithm (Eckstein, 2006), described by Avrutin *et al*, 2007 to estimate from sample orbits the number of connected components in the attractor.

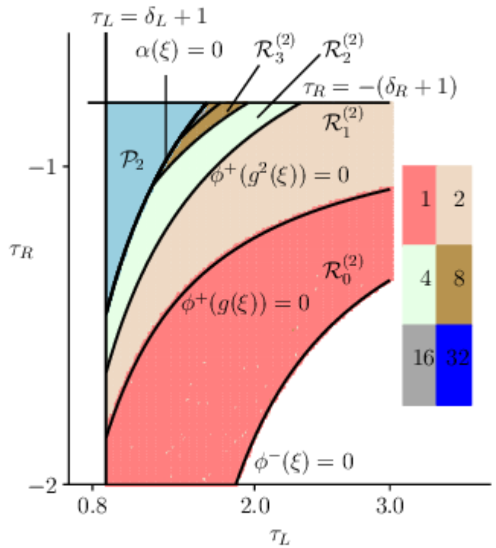

(a) $\delta_L = -0.1, \delta_R = -0.2.$

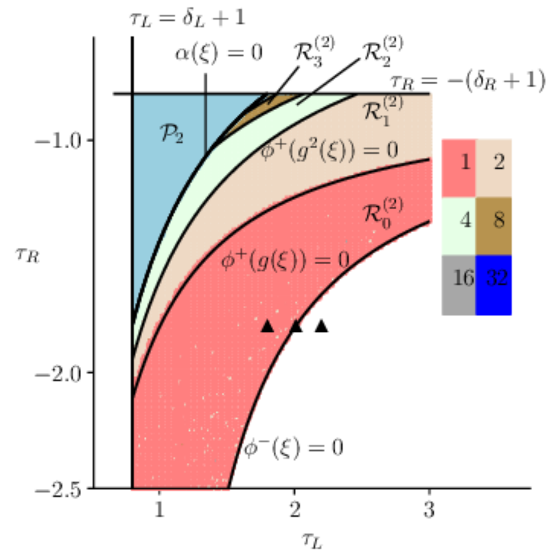

(b) $\delta_L = -0.2, \delta_R = -0.2.$

Numerics

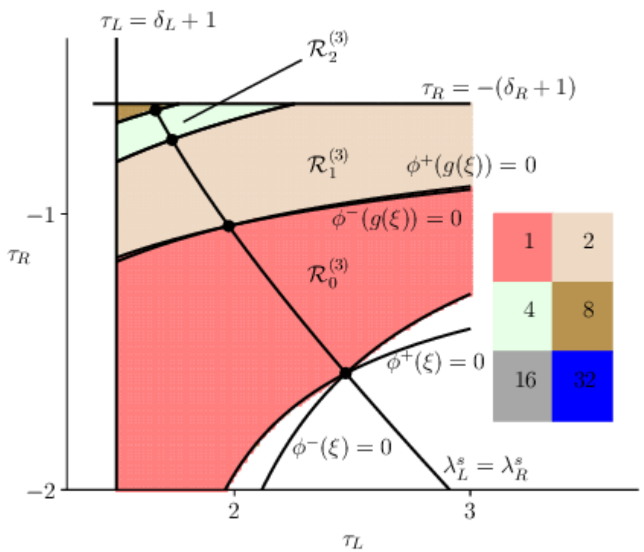

(a) $\delta_L = 0.5, \delta_R = -0.4.$

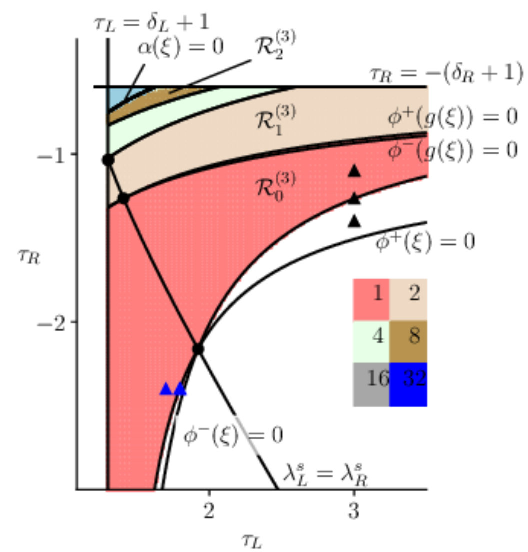

(b) $\delta_L = 0.3, \delta_R = -0.4.$

Numerics

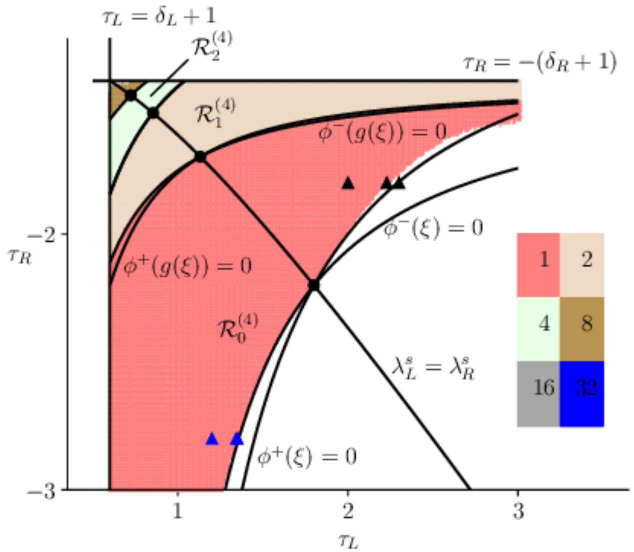

(a) $\delta_L = -0.4, \delta_R = 0.4.$

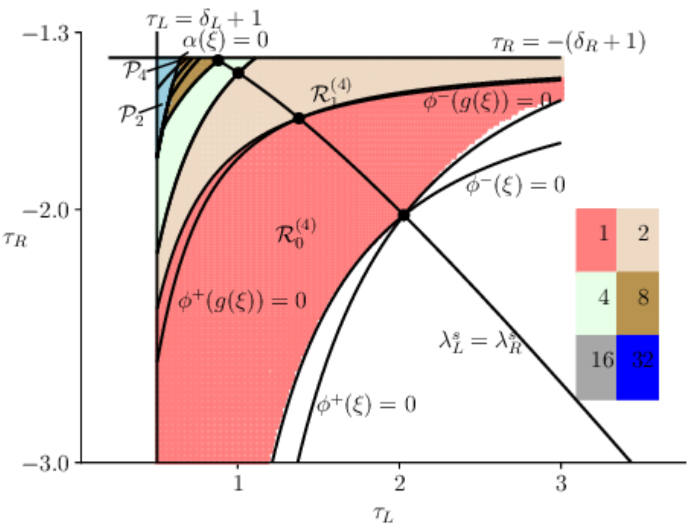

(b) $\delta_L = -0.5, \delta_R = 0.4.$

Numerics

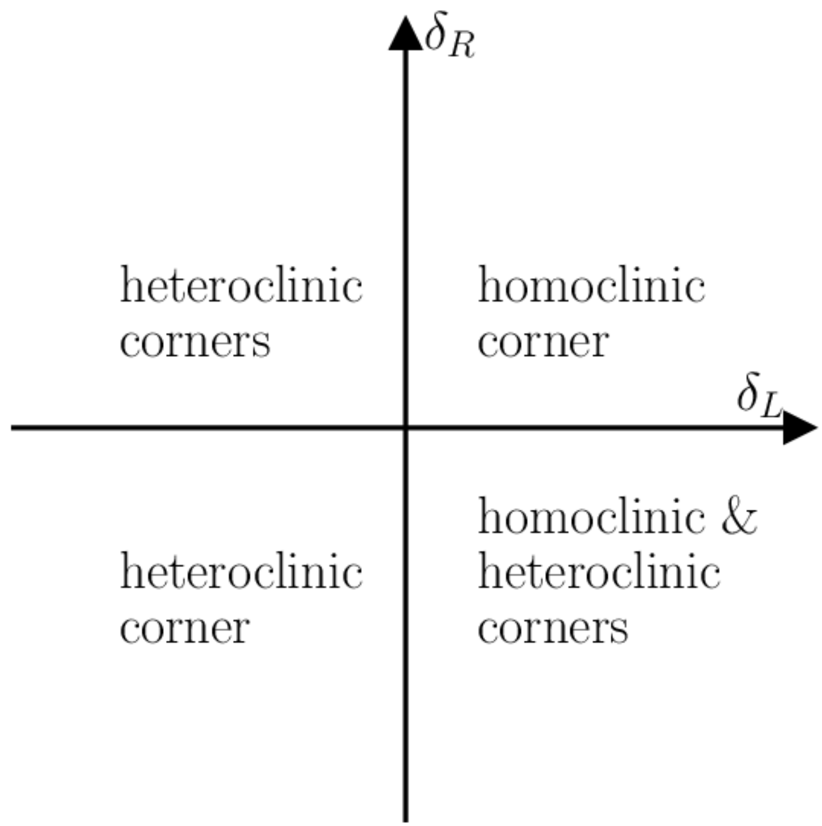

δ_R
δ_L
heteroclinic corners
homoclinic corner
heteroclinic corner
homoclinic & heteroclinic corners

Higher-dimensional setting

- Let $n \geq 2$. Suppose $\alpha > 1$ is an eigenvalue of A_L, and $-\beta < -1$ of A_R with multiplicity one, and all other eigenvalues of A_L and A_R have modulus at most $0 < r < 1$.

Theorem (Ghosh & Simpson, 2024)

Holding the above assumption and

$$r(n-1) < \frac{3}{7}\left(1 - \frac{1}{\alpha}\right), \qquad r(n-1) < \frac{3}{7}\left(1 - \frac{1}{\beta}\right),$$
$$r(n-1) < \frac{1}{10}\left(\frac{1}{\alpha} + \frac{1}{\beta} - 1\right),$$

then f has a topological attractor with a positive Lyapunov exponent.

Higher-dimensional setting

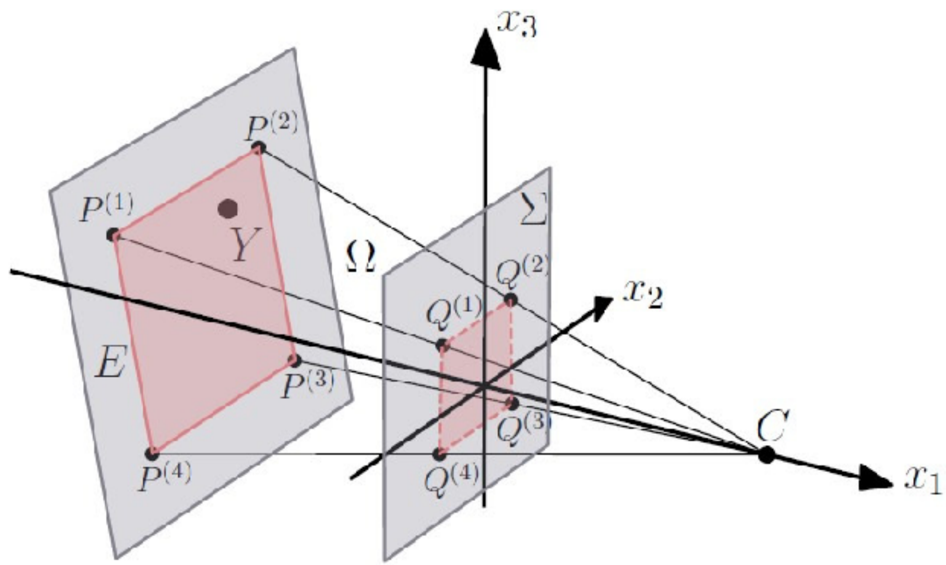

Figure: The construction of a forward invariant region Ω for $n = 3$.

Higher-dimensional setting

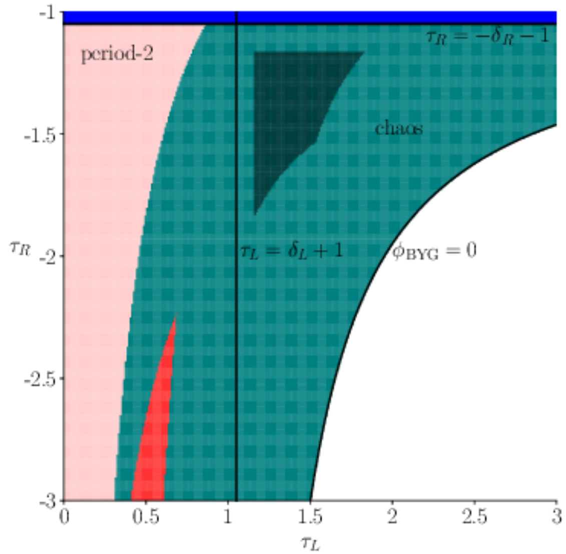

Figure: Robust chaos parameter region for the two-dimensional map, with our higher-dimensional construction portrayed on top of it. We chose $n = 2$ for simplicity.

Future Directions

- We expect our construction in the two-dimensional setting could be adapted to verify robust chaos beyond the boundaries reported.

Future Directions

- We expect our construction in the two-dimensional setting could be adapted to verify robust chaos beyond the boundaries reported.
- It would be interesting to see if renormalisation schemes based on other symbolic substitution rules can be used to explain parameter regimes where the BCNF has attractors with other numbers of components, e.g. three components.

Future Directions

- We expect our construction in the two-dimensional setting could be adapted to verify robust chaos beyond the boundaries reported.
- It would be interesting to see if renormalisation schemes based on other symbolic substitution rules can be used to explain parameter regimes where the BCNF has attractors with other numbers of components, e.g. three components.
- Maps with multiple directions of instability should be just as relevant, giving the possibility of so-called wild chaos, and it remains to treat these scenarios.

Future Directions

- We expect our construction in the two-dimensional setting could be adapted to verify robust chaos beyond the boundaries reported.
- It would be interesting to see if renormalisation schemes based on other symbolic substitution rules can be used to explain parameter regimes where the BCNF has attractors with other numbers of components, e.g. three components.
- Maps with multiple directions of instability should be just as relevant, giving the possibility of so-called wild chaos, and it remains to treat these scenarios.
- As one application I want to apply n–dimensional construction as the key space for an encryption scheme.

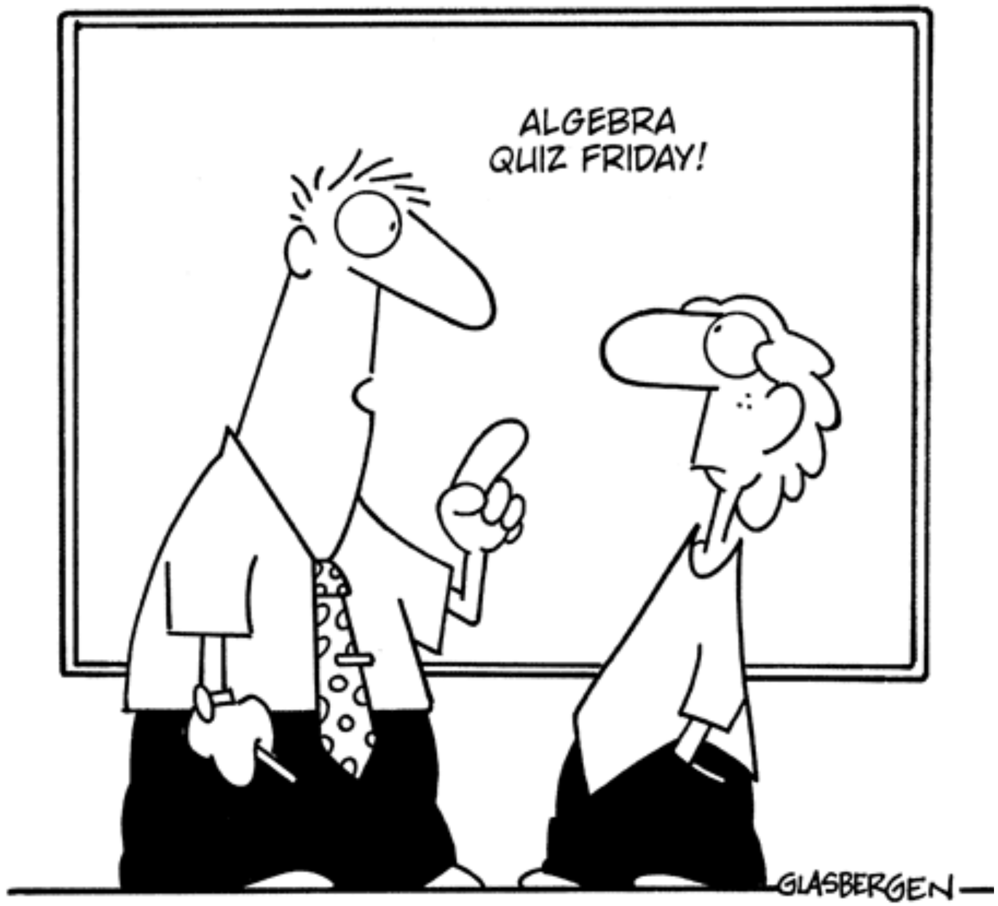

"It's important to learn math because someday you might accidentally buy a phone without a calculator."

The End

Thank you! Questions?